Structure of Amorphous Starch. 2. Molecular Interactions with Water

U. Trommsdorff* and I. Tomka

Institute for Polymers, Swiss Federal Institute of Technology Zurich, ETH-Zentrum, CH-8092 Zurich, Switzerland

Received December 9, 1994; Revised Manuscript Received May 23, 1995[⊗]

ABSTRACT: A detailed atomistic model for amorphous starch with water contents typical for this system at ambient atmospheric conditions was stimulated, extending the model for dry amorphous starch presented previously. The interactions of the molecules in this system were found to be dominated by the interactions of the hydroxyl groups of starch within themselves as well as with the water molecules. The possibility of forming hydrogen bonds was dramatically increased through the introduction of the small water molecules. On the macroscopic level this was reflected in the increase of the cohesive energy density up to 17×10^8 N/m^3 in the structures with 23% water, which was parallel to the increase in the density of *inter*molecular hydrogen bonds. With increasing water content, the starch chains were moved further apart and the interaction energy between them was reduced. Water was bound in the system with four hydrogen bonds, irrespective of whether the partner was a starch or a water molecule. The binding energy was constant with increasing water content. The model calculations confirmed that an excess energy is needed to evaporate water form the system. The mobility of the water molecules was found to be distributed broadly over 3 orders of magnitude in the correlation times, and the movement of the molecules was anisotropic. The calculation of the chemical potential of the water confirmed the high affinity of dry starch toward water.

Introduction

Starch has always been an important component in the diet of humankind, but it has also been used for nonfood purposes. The oldest known application dates back to 4000 B.C., when it served as an adhesive to cement together strips of Egyptian papyrus.[1] Starch from various plants can be transformed into a thermoplastically processable and biodegradable working material through a thermomechanical treatment using a suitable plasticizer.[2−5] However, the dependence of the material properties on the environmental conditions, in particular on the humidity of the atmosphere, has been the major drawback of its use. Starch is known to absorb considerable amounts of water[6,7] and thereby its properties, e.g., the glass transition temperature,[6−9] are changed. Because of their relevance in foods, starch−water systems are and have been extensively investigated (see, e.g., refs 10−12). Low humidity, for example, guarantees a longer shelf life of food products by preventing the deterioration due to the growth of microorganisms, but also keeps crackers from losing their mechanical properties, i.e., their crispiness. Thermoplastic starch is used today with success in combination with hydrophobic blending partners.[13]

The molecular interaction of water with the starch matrix is a longstanding matter of investigation. Experimental evidence has found this interaction to be very strong and localized during the early stages of sorption,[6,7,14] whereas at high water contents parts of the water molecules were found to exhibit liquid-like properties.[15,16] It was the aim of this study to investigate the role of the water as a plasticizer in dense amorphous starch. The strategy adopted here was to extend the atomistic model of dry amorphous starch presented previously[17] by incorporating different concentrations of water molecules. The approach allowed a molecular view of the interactions of the small water molecules with the starch chains. The moist model structures were furthermore compared to X-ray data by means of the differential radial distribution function, and some aspects of the mobility of water in the starch matrix were simulated and are discussed. Finally, an attempt was made to calculate the chemical potential of the water in amorphous starch.

Previous Work

At room temperature dry starch is well below its melting and glass transition.[7,8,18] The water molecules that are sorbed up to concentrations of ca. 1 H_2O per D-anhydroglucose unit (~10% by weight) show a sorption enthalpy that is 2.8 kcal/mol higher than the heat of condensation of pure water.[14] The starch matrix swells slightly, but less than would be expected from a linear combination of the respective densities of pure starch and water.[6,7] The mean correlation times of the movement of the water molecules, as evaluated from proton NMR relaxation time measurements, are of the order of magnitude of those in ice.[19] These observations suggest that the first water molecules undergo a strong and localized interaction with the starch matrix. The term "bound water" has often been used in this respect. Roosen[19] has shown that a distribution of correlation times of the water molecules exists even at such low levels of hydration and that their mobility increases with every water molecule that enters the structure.

At higher water contents, between approximately 1 and 3 H_2O per D-anhydroglucopyranose unit (~10−25% by weight), the excess sorption enthalpy decreases to a value[14] of 1.2 kcal/mol, the diffusion coefficient of water increases one order of magnitude to[19] ~10^{11} m^2/s, and the amorphous matrix becomes gradually plasticized, whereby the glass transition reaches room temperature in structures with ~18% of water.[7,8] This implies that the starch−water system is not at thermodynamic equilibrium at room temperature and low water content. In fact, the water sorption isotherm shows a hysteresis upon sorption and desorption.[6,7]

The mean mobility of the water gradually increases and the distribution of the mobilities is broad.[19] ^{2}H and

[⊗] Abstract published in *Advance ACS Abstracts,* August 1, 1995.

0024-9297/95/2228-6138$09.00/0

^{17}O NMR measurements reveal that long correlation times of "tightly bound" water exist,[20] whereas ^{1}H NMR measurements of Tanner[15] suggest a high mobility. This study shows, furthermore, that the water molecules reorient anisotropically in the starch structure. Also, measurements of the heat capacity of the starch–water system suggest that the water has liquid-like properties,[16] and near-IR measurements point to the existence of two broad categories of water in the starch matrix.[21]

At even higher water contents (>25%), a part of the water is observed to freeze upon cooling the system below 0 °C and the water in the structure becomes more and more indistinguishable from bulk water.[6]

Thermoplastic starch that has been destructurized with water as a plasticizer (in the following called destructurized starch) shows a somewhat smaller water sorption than native starch.[7] The shape of the isotherm and the results on the mobilities of the water molecules[19] are similar. Summarizing, it may be stated that experimental evidence is found for the water in a starch matrix to exhibit liquid-like and solid-like properties. A water sorption model which accounts for both forms has been proposed by Tomka[22] and applied to starch by Sala and Tomka.[7]

Computer simulation offers a tool to investigate the interaction of the water and the carbohydrate molecule from a molecular point of view. It has been shown that the conformation of small carbohydrates is sensitive to the nature of the solvent.[23–29] Eisenhaber and Schulz[30] found differences in the hydration shell of parallel and antiparallel double helices of amylose by a Monte Carlo simulation. These simulations demonstrate the importance of the interactions of the polar hydroxyl groups of these molecules, offering numerous hydrogen-bonding possibilities among themselves as well as with the solvent molecules, particularly with water.[31] Water can even stabilize certain conformations by acting as a bridging molecule.[25] The network of hydrogen bonds is dynamic, and typical bonding sites near the hydroxyl groups[32–34] were occupied during the simulation time (50 ps) by *exchanging* water molecules (typically after 6 ps). Similar behavior has been simulated for the cellobiose molecule in water.[35] Hydrogen bonds exist in a variety of geometries including three-center bonds.[31] The occurrence of three-center bonds has been observed by neutron diffraction in cyclodextrin crystals and was found also with atomistic simulations.[36] Because of the long-range interaction of the polar hydroxyl groups, the choice of the force field used in the simulation has to be made with care. It has been pointed out by Brady and Schmidt,[37] who closely investigated the hydrogen bonds between the saccharide and the solvent, that effects of the solvation on the conformation of the molecule can be sensitive to the force field used.

The atomistic model of starch[17] provided an opportunity to investigate the starch–water interactions in the dense state, for which no simulations have been found in the literature, and to contribute to the clarification of the role of the water.

Model for "Moist" Amorphous Starch

For this study the atomistic model for dry amorphous starch[17] has been extended. The model used the basic assumptions of the Theodorou–Suter method for the simulation of glassy polymers:[38] (1) the glass was seen as a state of frozen-in liquid disorder where the temperature enters only through the specification of the density and (2) the polymer was represented as an ensemble of microstructures, each of which is in a local minimum of the potential energy. The system was modeled in cubic cells with periodic continuation conditions and the interactions between all atoms were treated explicitly. It was further assumed that amorphous starch can be simulated by neglecting chain branching.

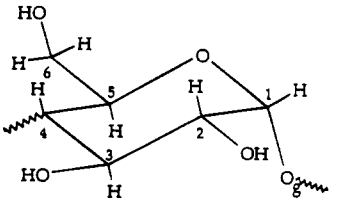

Figure 1. Repeating unit of starch: α-D-anhydroglucopyranose.

Table 1. Water Content in 100 × $g_{H_2O}/(g_{H_2O} + g_{starch})$, Number of Water Molecules per Microstructure, and Densities of the Simulated Structures[a]

no. of microstructures	% wt of water	water molec/ structure	density (g/cm^3)	T_g (°C)
3	0.0		1.50	>180
3	8.2	64	1.50	135
3	14.8	125	1.47	80
3	23.1	216	1.42	30
1	32.2	343	1.36	<room temp
1	100.0	260	0.98	

[a] For comparison, the models of pure starch and water are included. Glass transition temperatures, T_g, of the destructurized starch, with water contents corresponding to those of the simulated structures, have been taken from Benczédi.[41] The density of pure water at 300 K has been taken from the *Handbook of Chemistry and Physics*.[56]

The construction of the microstructures consisted essentially of three steps: (1) an initial guess structure was constructed at a density of 1.0 g/cm^3 by building up a chain of α-D-anhydroglucose units (Figure 1) with the energy-biased "polymerization" method,[17] (2) the density was adjusted by molecular dynamics by selecting the proper pressure (*NPT*), and (3) the structures were relaxed to minimal potential interaction energies by energy minimization. For the energy minimization and molecular dynamics, the Discover modeling software of BIOSYM Technologies (Version 2.9) with the PCFF91 force field[39,40] was used. For details on the model construction and the choice of the force field, see Trommsdorff and Tomka.[17]

Different ways can be imagined to fit water molecules into "dry" model structures. However, there is no special method that would be based on firm physical background *and* that could be realized with reasonable computer time. Here it was chosen to distribute the water molecules homogeneously in the same initial guess structures that previously had been used to generate the dry starch model (after step 1). With this method, three starch–water systems having different water contents (3 microstructures each) were constructed at 300 K. Their densities correspond to those measured for the system of destructurized starch with water.[41] Note that the experimentally determined (DSC) glass transition temperature, T_g, of destructurized starch lies in the region of room temperature for the system with 23% water. One additional microstructure with a higher water content was constructed for the investigation of the water mobility. Pure water was also simulated. Table 1 summarizes the water content, the number of water molecules, the densities of the model structures, and the corresponding experimentally

measured glass transition temperatures[41] of destructurized starch. The degree of polymerization of the starch chain was 80 in all structures.

Three further points have to be noted. First, for economical reasons the duration of the *NVT* molecular dynamics during the relaxation step of the model construction was limited to 20 ps. The effect of a longer (80 ps) simulation time was small on the potential energy and the cohesive energy density of the minimized structure as well as on the conformation angle distribution. Second, the experimental densities could not be reached by simply applying *NPT* molecular dynamics at a pressure that just corrected for the cutoff used to calculate the energy expression, but higher pressure had to be applied. Compared to the "dry" systems, however, the pressure was much smaller. It has been discussed[17] that an adjustment of the force field parameters to fit carbohydrates could solve this problem. Third, to improve the statistics, a large number of microstructures should be generated; however, limits had to be set to match the currently available computer power.

X-ray Scattering Experiments

X-ray scattering experiments were performed on samples of destructurized starch with different moisture contents, monitoring structural changes that accompany the change of the water content. The differential radial distribution function[42] $4\pi r^2\Delta\varrho^x(r)$ was evaluated, which describes the radially averaged difference $\Delta\varrho(r)$ between the local and the mean density of atoms that are found at a distance r around an arbitrary atom. At high distances, this function tends to zero; i.e., the local density corresponds to the mean atomic density in the system. At distances of a few atomic radii, however, the local density is determined by the *inter-* and *intra*molecular distance relations of the neighboring scatterers. The procedures used have been described in detail in the previous contribution.[17]

Destructurized starch was produced from native potato starch (Firma Blattmann & Co., Wädenswil CH), which showed the high-temperature transition at 181 °C (at 18% water; for the interpretation of this transition, see Willenbücher[5]) and an intrinsic viscosity of 314 mL/g. The starch (27% water) was processed in a BUSS extruder (temperature: 101−102 °C; introduced mechanical work: 0.21−0.24 kwh/kg) and granulated. The intrinsic viscosity was 115.6 mL/g after the melting process.

For the "dry" sample the granulate (18% water) was molten and formed to a platelet with 1 mm thickness in a press at 130 °C. Thereafter it was dried to constant weight (approximately 2 months) in a vacuum oven at 80 °C over P_2O_5. The residual water content was less than 0.5%. The X-ray scattering experiments were performed in a SCINTAG PADX θ/θ diffractometer using a solid-state detector for Cu Kα radiation. The measurement was performed at 25 K in a low-temperature attachment with a closed-cycle helium cryostat. The angular range (2θ) was 2−140°, the step size was 0.05°, and the recording time per step was 30 s.

For the moist samples, the granulate of destructurized starch was ground in a mortar to a fine powder, and the water contents of the three samples, after storing them for 2 months in exsiccators at different humidities, were 4.9, 12, and 18.35% (weight). The samples were placed in Lindemann tubes with a diameter of ca. 2 mm, and the tubes were sealed to prevent a change of the water content during the exposure. The X-ray scattering experiments were performed in a Philips PW1380 goniometer with a Syntex P2 X-ray generator and a proportional counter. The data were recorded at room temperature from 5 to 155° (2θ) with a step size of 0.02° and a recording time of 10 s per step. The samples were completely bathed in the X-ray beam.

For all cases, the measurement was repeated at the same conditions but with an empty cell to record the scattering from air and from the sample holder.

To calculate the differential radial distribution function $4\pi r^2\Delta\varrho^x$ of a structure from scattering data, it was necessary to provide the coherent intensity, $I(q)$, in absolute units. Therefore, the measured intensity $I_{meas}(q)$ and to be corrected for the "empty cell" scattering $I_{add}(q)$, polarization $P(q)$, absorption $A(q)$, and incoherent scattering $I_{inc}(q)$ and to be scaled (K) to absolute units (e.g., Klug[42] and Alexander[43]). The correction for multiple scattering in the sample was omitted because it is of the order of 5% (at high scattering angles) of the intensity only.[44] The measured intensity was

$$I_{meas}(q) = I_{add}(q) + KP(q)A(q)[I(q) + I_{inc}(q)]$$

The evaluation of the individual terms and the calculation of the differential radial distribution function were described in the previous contribution.[17] The correction for absorption and polarization had to be adapted to the conditions of the measurement,[42] i.e., to transmission and to crystal monochromaticized incident radiation. Furthermore, the absorption factor for cylindrical samples of Weber[45] was applied.

Evaluation of the Chemical Potential of Water in the Model Structures

The chemical potential μ_A of component A in a system containing N_A particles of the sort A and N_B particles of the sort B at constant volume V and temperature T can be written as (for a detailed derivation, see Ben-Naim[46])

$$\mu_A = RT\ln\left(\frac{\Lambda_A^3}{q_A}\frac{N_A^{id.gas}}{V}\right) + RT\ln\left(\frac{V}{N_A^{id.gas}}\frac{(N_A+N_B+1)}{V}\right) - RT\ln\langle\exp(-U_A/RT)\rangle \quad (1)$$

Λ_A is the de Broglie wavelength, q_A is the internal partition function of the particle A, and U_A is the potential energy of interaction of a test particle of species A with the system of A and B particles. The angular brackets denote a canonical ensemble average. $N_A^{id.gas}$ is the number of A particles in the volume V in the ideal gas state. R is the gas constant. This redundant expression of the chemical potential was used to identify the terms with the usual thermodynamic formulation:

$$\mu_A = \mu_A^\circ + RT\ln a_A \quad (2)$$

The chemical potential of A in the ideal gas state is denoted by μ_A° and corresponds to the first term of eq 1, whereas the term with the thermodynamic activity a_A can be identified with the sum of the second and third terms.

For the derivation of eq 1, it has been assumed that the addition of one particle is an infinitesimal change of the total number of particles, $N_A + N_B$, in the system, that the potential energy of the system can be described by the interactions of pairs of atoms, and that the rotational and internal degrees of freedom of A particles are not affected by the system. The first two terms of eq 1 can be calculated readily if the density of the system as a function of the content of A is known. The last term is also called the excess chemical potential[48] μ_A^{exc}

$$\mu_A^{exc} = -RT\ln\langle\exp(-U_A/RT)\rangle \quad (3)$$

At low concentrations of a gaseous solute A, the value of $\langle\exp(-U_A/RT)\rangle$ is equivalent to the Henry's constant

in units of [cm³(STP)/(cm³ atm)], i.e., the number of solute molecules per unit volume of solution in equilibrium with solute ideal gas at standard conditions of 1 atm and 273 K.

For the evaluation of the excess chemical potential of water in starch, the "test particle insertion method" of Widom[47] was used. It involved the sampling and averaging of the interaction energy of a particle (water) inserted at different points into an equilibrium configuration of the system (starch + water). At every grid point i the potential energy of interaction U_{ij} of the test water with all the other water and starch molecules in the system was evaluated for a number N_{ori} of orientations j of the water molecule and therefore

$$\langle \exp(-U_w/RT) \rangle = \frac{1}{N_{grid}} \sum_{i}^{N_{grid}} \frac{1}{N_{ori}} \sum_{j}^{N_{ori}} \exp(-U_{ij}/RT) \quad (4)$$

To speed up the computation, the test water molecule was rotated around the center of the oxygen atom instead of around the center of mass. These two are displaced from each other by less than 1/10 of an angstrom. The number of orientations was restricted to 500 at each grid point. Higher numbers of orientations did not affect the result by more than 1%.

The size of the grid on which the water molecule was placed was chosen to be 0.5 Å. Test runs with half of this size indicated a difference in the result of only 1–2%; however, the time to calculate the chemical potential with the finer grid was 8 times higher.

The averaging of the excess chemical potential of water over a number N_{cubes} of microstructures was done as follows:

$$\overline{\mu^{exc}} = -RT \ln\left\{ \frac{1}{N_{cubes} N_{grid}} \sum_{i}^{N_{cubes} N_{grid}} \frac{1}{N_{ori}} \sum_{j}^{N_{ori}} \exp\left(-\frac{U_{ij}}{RT}\right) \right\} \quad (5)$$

Results and Discussion

Pure Water. A major difficulty in the design of water models is due to the strong and complex molecular interaction, which gives rise to the extraordinary properties of water. Several water models with different effective pair potentials have been proposed;[49] however, the PCFF91 force field provides its own parameters for water derived from quantum mechanical computations. Therefore, some properties of the pure liquid and of energy-minimized liquid water were simulated. It was found that the chosen force field gives an accurate representation of pure water in terms of the density, the cohesive energy density, and hydrogen bonding. As a measure of the mobility of the water molecules, the self-diffusion coefficient was evaluated to be 7×10^{-9} m²/s, which is in the correct order of magnitude (experimental value:[50] 2.3×10^{-9} m²/s).

Measured and Modeled Differential Radial Distribution Function $4\pi r^2 \Delta\varrho^x(r)$. The coherent part of the scattered radiation and the differential radial distribution functions of amorphous thermoplastic starch at different water contents are shown in Figures 2 and 3. The intensity curves (Figure 2) of the moist samples showed a broadened first and an increased second maximum. (Note that the lower noise of the signal of the "dry" sample is due to the different measuring conditions.) The differences, however, in the differential

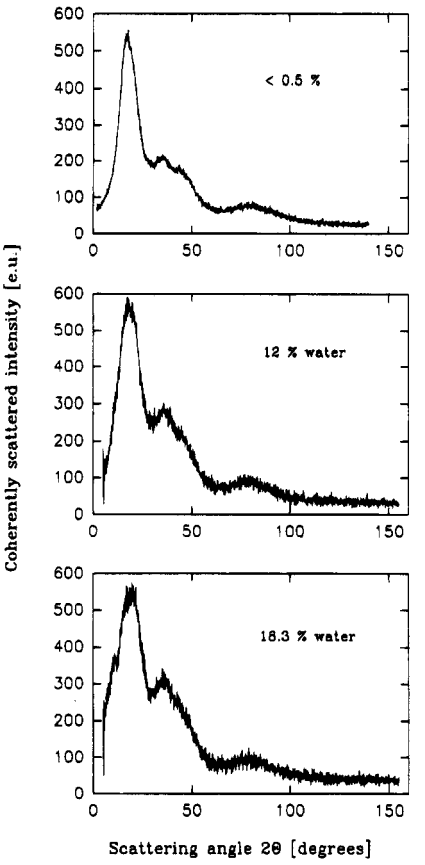

Figure 2. Intensity of coherent scattering measured by X-ray diffraction for the samples of destructurized starch at different water contents.

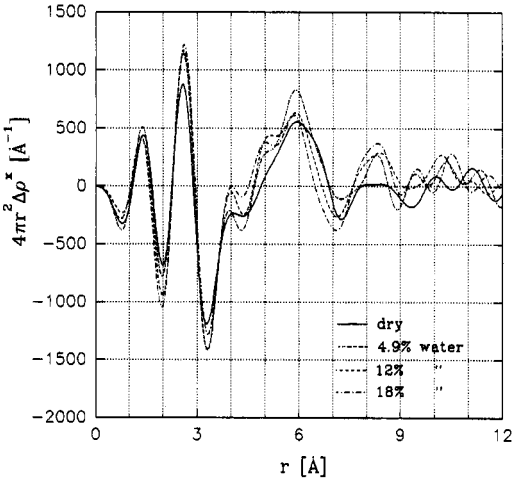

Figure 3. Differential radial distribution functions calculated from the measured X-ray scattering of samples of destructurized starch at different water contents.

radial distribution functions of the two moist samples and the dry sample (Figure 3) seemed to be small. There was no change with the water content of the positions of the first peaks up to 6 Å. A small increase in peak height was found at 4, 5, and 8 Å.

Figure 4 shows the $4\pi r^2 \Delta\varrho^x(r)$ of the measured sample with 12% water together with the one from the model structure with 14% water. (For the details of the evaluation of this function from the model structures, refer to the previous contribution.[17]) The agreement between experiment and model was good for the position of the first two peaks, which mainly describe the distances between the chemically bonded atoms. The lower and broader first peak of the experimental

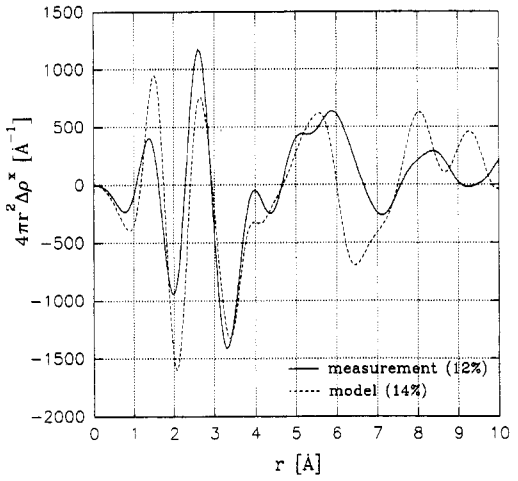

Figure 4. Comparison of the differential radial distribution function calculated from the model structure with 14% water and from the experimental data of the sample with 12% water.

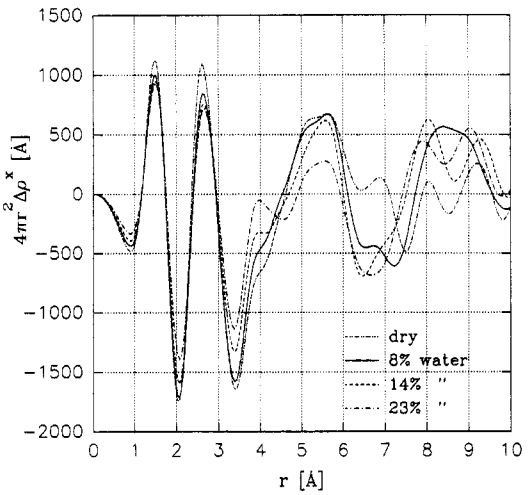

Figure 5. Differnetial radial distribution functions calculated from the model structures with different water contents.

$4\pi r^2\Delta\varrho^x(r)$ can be attributed to the limited scattering angle region.[43] The position of the peak at 4 Å was reproduced correctly by the model, and an increase of this peak with the water content was found, as shown in Figure 5. At distances higher than 4.5 Å, there was qualitative agreement. Similar to the experimentally determined differential radial distribution functions, the changes with the water content for the modeled $4\pi r^2\Delta\varrho^x$ were small (Figure 5) up to 6 Å. At higher distances, the statistics became affected by the small size of the model structures.

From these findings it can be concluded (1) that the modeled structures reproduce the measured differential radial distribution function of wet amorphous starch up to 5.5 Å and (2) that the water content has a small effect on the structure of amorphous starch as measured by wide-angle X-ray diffraction.

Structure and Hydrogen Bonding. From the results on the structure of the dry amorphous starch,[17] it is expected that again the hydrogen bonding is a key feature of the interactions of the molecules, all the more as through the introduction of water the hydrogen-bonding possibilities are augmented. An influence of the water content is to be expected on the interactions of the starch chain with the surrounding molecules (*inter*molecular structure), as well as on the conformation of the chain itself (*intra*molecular structure).

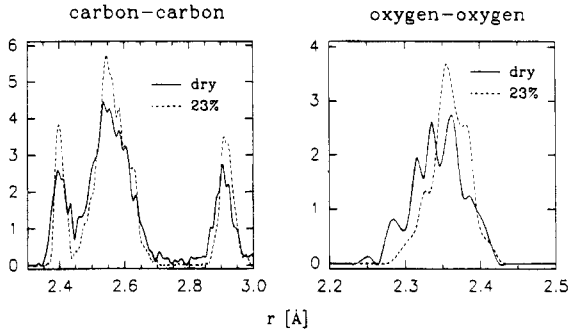

Figure 6. Enlarged sections of the *intra*molecular carbon–carbon and oxygen–oxygen distribution function of the structures with 0 and 23% water.

Table 2. Contributions of the Internal Degrees of Freedom to the Potential Energy in kcal/mol of the Starch Molecule (Consisting of 80 Repeat Units of α-D-Anhydroglucose) in the Starch–Water Model Structures at Different Water Contents (Mean Values and Standard Deviations)

energy	dry	8% water	14% water	23% water
E_{bond}	107 ± 2	114 ± 3	117 ± 2	126 ± 2
E_{angle}	833 ± 1	824 ± 22	790 ± 14	746 ± 7
E_{tors}	−2256 ± 10	−2313 ± 16	−2361 ± 14	−2398 ± 5
E_{cross}	−479 ± 7	−483 ± 17	−465 ± 14	−454 ± 6
E_{int}^{tot}	−1795 ± 14	−1858 ± 13	−1919 ± 14	−1979 ± 5

As in the previous contribution,[17] a geometrical definition for the hydrogen bonds has been used:

(1) All hydrogens belonging to hydroxyl groups and all oxygen atoms in the starch molecules were considered.

(2) A pair of a hydrogen atom and an oxygen atom were considered to be hydrogen bonded if their distance is smaller than 2.25 Å. Pairs with higher distances (2.25–2.65 Å) were also considered hydrogen bonded if they form part of a three-center bond.

"Three hydrogen bonds per repeat unit" (or per molecule) signifies that each of these repeat units was connected by three hydrogen bonds to some others.

(a) Intramolecular Structure. The increase in the water content influenced the internal degrees of freedom of the starch molecule. Table 2 shows their contribution to the potential energy of the structure according to the PCFF91 force field. It consists of terms that describe the deformation of bond lengths (E_{bond}), bond angles (E_{angle}), and torsion angles (E_{tors}). It contains also cross terms (E_{cross}) which link these deformations. The contributions of the angles and torsion angles diminish with increasing water content, whereas the bond and the cross terms augment slightly. The sum of these terms, E_{int}^{tot}, is reduced with increasing water content—the starch chain is reaching a conformation of lower potential energy.

The change in the angles can be seen in the *intra*molecular pair distribution function. Figure 6 shows a section of the *intra*molecular carbon–carbon pair distribution function that corresponds to distances within the repeat unit (see Figure 1). The peaks are sharper in the structure with water and, above all, the tails at the lower distances are missing. (The first two peaks correspond to distances between carbons that are separated by two bonds, and the third peak corresponds to the distance within the ring between opposite atoms.) The same was true for the peak at 2.35 Å in the oxygen–oxygen pair distribution function shown in Figure 6, which corresponds to the distance between the ring and the glycosidic oxygen. On one hand, these effects could

Table 3. Mean End-to-End Distance $r_{end\text{-}to\text{-}end}$ of the Starch Chains (Initial Guess: 80.4 Å) and Distribution of the Conformation Angle Pairs ϕ/ψ among the Regions I and II of the Dimer Conformation Map[17] (the Variation for the Different Microstructures Is Less Than 4%)

	water content (%)		
	8	14	23
$r_{end\text{-}to\text{-}end}$ (Å)	70.6 ± 23	76.0 ± 40	78.9 ± 29
% of ϕ/ψ pairs in I and II, respectively	23/77	26/74	23/77

be caused by the force field, i.e., by the high internal pressures in the structures at low water content. On the other hand, changes in the conformation of the molecules due to changes in the water content are often observed in crystalline biopolymers.[51] Here it could be argued that the strong interactions between the hydroxyl groups in the starch chains lead to local distortions that would be diminished by the insertion of small and relatively mobile water molecules. Furthermore, the number of hydrogen bonds *within* each repeat unit, which was approximately 1 in the dry structures,[17] was reduced to half at the highest water content, which also could cause a relaxation of the geometry of the repeat unit.

The mean end-to-end distances of the starch chains and the distribution of the conformation angles at the glycosidic linkage among the two major conformation angle regions I and II (see previous contribution[17]) are displayed in Table 3. The extension of the chain depends on the degree of compression during the preparation of the microstructures. Since the density of the starch–water system decreases with the water content, structures with high water content have been compressed less. The change in the conformation angle distribution due to the introduction of water was small and not systematic.

(b) Intermolecular Structure and Hydrogen Bonding. The introduction of the small water molecules into the amorphous starch structures led to changes in the distance correlations between the starch chains. With increasing water content the starch chains moved further apart, as can be seen in Figure 7, where enlarged sections of the carbon–carbon pair distribution functions for the structures at different water contents are shown. The overall change in the nearest neighbor distance from the dry structure to that with 23% water was ca. 0.4 Å. The intermolecular pair distribution functions showed peaks at distances characteristic for hydrogen bonds, as were found previously in the dry structures[17] (not shown). Counting the number of hydrogen bonds made by the repeat units of starch with other repeat units, a decrease of not only *inter*molecular but also of *intra*molecular hydrogen bonds was found (Figure 8). Clearly, the introduction of the small water molecule widened the structure and reduced the *inter*molecular and the *intra*molecular connections between the starch chains.

The number of hydrogen bonds per water molecule and per repeat unit of starch is shown in Figure 9. As might be anticipated, every water molecule made four hydrogen bonds to the neighboring molecules at high water contents. However, already at low water contents nearly four hydrogen bonds per water molecule were found. This may be explained by the high flexibility of the small water molecule and by the high number of hydrogen-bonding sites offered by the starch molecule. The number of *inter*molecular hydrogen bonds per repeat unit of starch was sharply increasing with

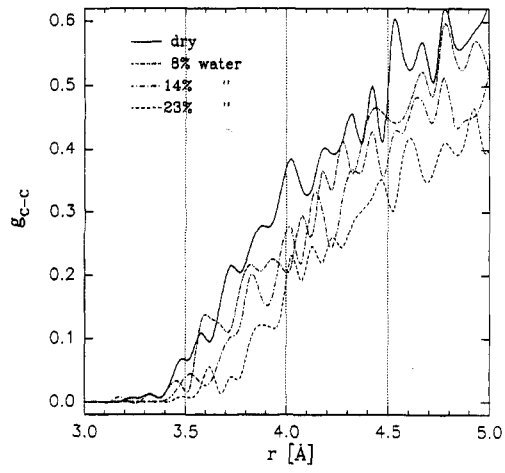

Figure 7. Enlarged section of the *inter*molecular carbon–carbon distribution function of the structures at different water contents.

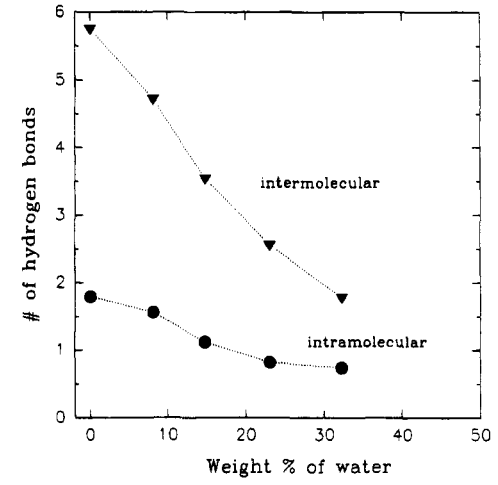

Figure 8. Number of *inter*- and *intra*molecular hydrogen bonds between repeat units of starch as a function of the water content in the model structures.

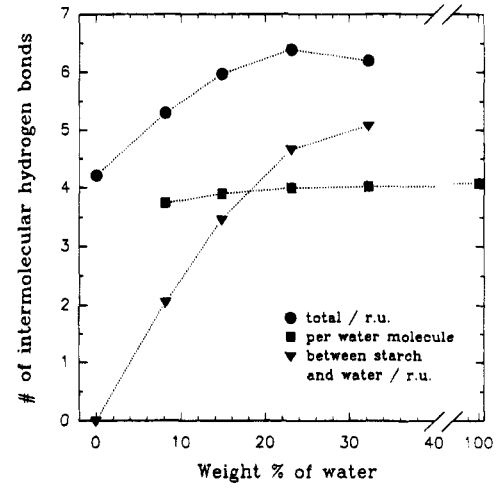

Figure 9. Number of *inter*molecular hydrogen bonds per repeat unit (r.u.) (total and with water molecules only) and per water molecule as a function of the water content in the model structures.

increasing water content due to the increase in the number of hydrogen bonds that starch forms with water molecules (Figure 9). Figure 9 further suggests that at higher water contents a saturation at about 7 *inter*molecular hydrogen bonds per repeat unit of starch is reached. (Note that the slightly lower value of the

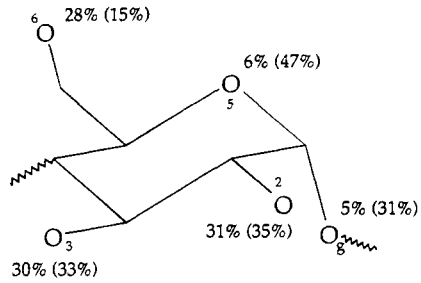

Figure 10. Distribution of hydrogen bonds among the individual oxygens of a repeat unit of starch. Mean values were taken over the 3 times 80 repeat units in the model structure with 14% water. Values in parentheses: fraction of *intra*molecular hydrogen bonds.

structure at the highest water content probably can be ascribed to the fact that it was determined from *one* microstructure only.)

These findings show that, similar to the dry amorphous starch structure, the main *inter*molecular structuring element is hydrogen bonding. However, with increasing water content the starch chains were to a lesser extent directly bound to each other, but through bridging water molecules.

With increasing water content, the main changes in the structures occurred at distances corresponding to hydrogen bond distances, i.e., between 2 and 3 Å. In the same distance range major *intra*molecular correlations were also found (Figure 6). This fact offers an explanation for the small change with water content that had been found in the differential radial distribution functions. With wide-angle X-ray scattering experiments there is no hope in getting better resolution of such small differences. With neutron scattering the contrast could be enhanced, but not enough to justify the experimental effort. The electron density of starch is approximately 50% higher than that of water, whereas the scattering length density of starch can be increased to be ca. 10 times higehr than that of water. This contrast would be reached by replacing nonhydroxyl hydrogens with deuterium and using ordinary water as solvent.

In Figure 10 the distribution of hydrogen bonds among the individual oxygen atoms of the repeat unit of starch is displayed for the structure at the intermediate water content of 14% by weight. (Note that for this calculation the hydrogen bonds within the repeat unit have been taken into account, too.) Approximately 90% of all hydrogen bonds were formed by the three hydroxyl groups. As might be anticipated, the OH(6) hydroxyl, which is the least sterically hindered group, made the most *inter*molecular hydrogen bonds. The ring oxygen made most *intra*molecular bonds. The distribution of the hydrogen bonds on the different hydroxyl groups and their number per group was constant within 1–2% in the moist starch structures (Table 4). The dry starch structure, however, contained fewer hydrogen bonds. Similar results on the distribution of hydrogen bonds have been found in simulations of maltose (dimer of α-D-anhydroglucose) in water.[37] The number of hydrogen bonds, however, was higher, as would be expected for a small molecule in solution.

Similar to the dry structures, the geometry of the hydrogen bridges was variable and only restricted by repulsive interaction of the atoms involved (Figure 11).

(c) Hydrogen Bonds to Two or More Partners. Table 5 displays the amount of oxygens and polar hydrogens that are hydrogen bonded to *two* or more partners. An oxygen atom can be an acceptor of two hydrogen bonds. This situation was found for 20% of all the oxygen atoms belonging to hydroxyl groups and seemed to be independent of the water content. This was less than for small polysaccharide molecules in water,[37] where almost three hydrogen bonds were found for each hydroxyl group. The amount of "double" hydrogen bonds made by the ring and the glycosidic oxygen was small and decreased with water content. On the other hand, the fraction of oxygen atoms of the water molecules that are acceptors of two or more hydrogen bonds increased with water content to reach 88% in the pure energy-minimized liquid water structure. Furthermore, an increasing amount of oxygen atoms belonging to water formed more than *three* hydrogen bonds (<5% in the starch–water system, but 14% in the pure water). Oxygen atoms belonging to starch were

Table 4. Number of Hydrogen Bonds for Each Individual Oxygen Atom in the Starch Repeat Unit[a]

	water content (%)			
	0	8	14	23
OH(2)	2.4 ± 0.2	2.6 ± 0.1	2.6 ± 0.2	2.5 ± 0.1
OH(3)	2.4 ± 0.02	2.4 ± 0.1	2.5 ± 0.03	2.5 ± 0.04
OH(6)	2.1 ± 0.1	2.4 ± 0.1	2.4 ± 0.03	2.4 ± 0.1
O(5)	0.5 ± 0.07	0.5 ± 0.07	0.5 ± 0.1	0.5 ± 0.05
O_g	0.4 ± 0.03	0.5 ± 0.02	0.4 ± 0.07	0.4 ± 0.04
total	7.8 ± 0.2 (54%)	8.4 ± 0.3 (64%)	8.4 ± 0.1 (71%)	8.3 ± 0.1 (77%)

[a] Mean values and standard deviations taken over all repeat units in the model structures. Values in parentheses: fraction of *inter*molecular hydrogen bonds.

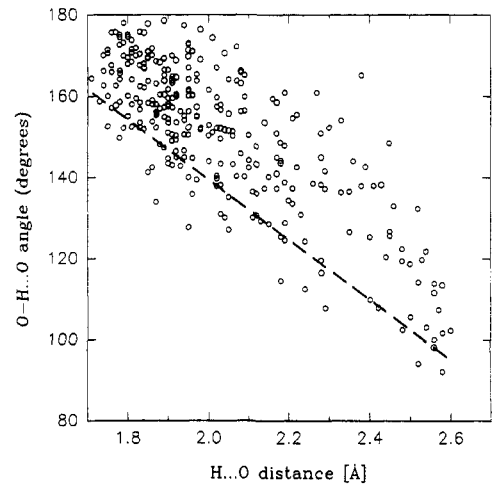

Figure 11. Hydrogen bond angles O–H···O in degrees plotted against the corresponding hydrogen bond distance O···H in angstroms in one of the microstructures with 8% water. Dashed line adapted from Savage and Finney.[57]

Table 5. Fraction of Oxygens and Polar Hydrogens in the Starch–Water System That Are Hydrogen Bonded to Two or More Partners (Mean Values and Standard Deviations[a])

water content	$O_{hydroxyl}$	$H_{hydroxyl}$	$O_{ring}O_{glyc}$	O_{water}	H_{water}
0.00	21 ± 2	39 ± 2	6 ± 1		
0.08	18 ± 2	33 ± 3	5 ± 2	31 ± 6	15 ± 1 (0.2)
0.14	20 ± 2	25 ± 2	3 ± 1	33 ± 1	14 ± 1 (0.4)
0.23	20 ± 2	19 ± 1	3 ± 1	44 ± 3	10 ± 1 (0.5)
0.32[b]	20[b]	15[b]	2[b]	53[b]	7[b] (0.4)
1.00				88[b]	3[b]

[a] In parentheses: *number* of water-to-starch bifurcated donor hydrogen bonds per repeat unit of starch (see text). [b] Note that only one microstructure was calculated for these systems.

rarely found to form more than two hydrogen bonds (<1%).

Because the starch molecule contains only three hydrogen-bond donors but five acceptors per repeat unit, hydroxyl hydrogens were found that make two bonds. This type of hydrogen bond is called the "bifurcated donor or three-center hydrogen bond"[52] and has been systematically investigated in saccharide molecules by Ceccarelli et al.[53] The number of hydrogen atoms of starch that were involved in bifurcated donor hydrogen bonds decreased with increasing water content from 39% in dry starch to 15% in the structure with the highest water content. Jeffrey and Mitra[54] have found ca. 20% of bifurcated donor bonds in crystal structures of small saccharide molecules. Koehler et al.[36] pointed out that in solution more different bifurcated donor bonds exist, but their population is lower than in the crystal. From the results shown above, it can be concluded that the number of bifurcated donor hydrogen bonds depends on the water content of the system. It decreased with increasing amounts of water in the structure.

Due to the hydrogen-bond donor deficiency of starch, the hydrogen atoms of water were also engaged in more than one bond in the starch–water system. The fraction of hydrogens of water that act as bifurcated donors decreases with water content and is approximately 3% in the pure energy-minimized liquid water structure. The absolute number of situations where the starch molecule formed two bonds to the same hydrogen atom of a water molecule increased with the water content.

Cohesive Energy Density of the Starch–Water System. In the dry amorphous starch model structures it had been found that the cohesive energy density is proportional to the density of *inter*molecular hydrogen bonds[17] (the latter had been modified through the conformation of the chain). In the "moist" amorphous starch structures, the density of *inter*molecular hydrogen bonds was increased by raising the water content (Figure 12a). Again, the cohesive energy density—the total *inter*molecular potential energy per volume—of the starch–water system was proportional to the *inter*molecular hydrogen-bonding density (Figure 12b). Therefore, it increased with increasing water content (from 7.8×10^8 J/m^3 in the dry structures to 17×10^8 J/m^3 in the structure with 23% water) and the values for the moist structures were within 20% of the experimental results.[41] However, dividing the total *inter*molecular energy into separate contributions from the starch and the water molecules, it was found that the *inter*molecular energy between the starch chains decreased with increasing water content (Figure 13). This is equivalent to the observation that the *inter*molecular hydrogen bonds between the starch chains were reduced when water was introduced and can again be interpreted as a weakening of the structure. However, in line with increasing the number of hydrogen bonds per repeat unit of starch (Figure 9), the energy necessary to take one starch chain out of the system was increasing (Figure 13). Therefore, with respect to the *inter*molecular energy, the structure was *not* weakened through the introduction of water molecules.

Binding Energy of the Water Molecules. To address the question of whether some water molecules are more bound in terms of energy than others, the binding energy was evaluated for all water molecules. Figure 14 shows the histograms of the binding energy at the different water contents and Table 6 presents the

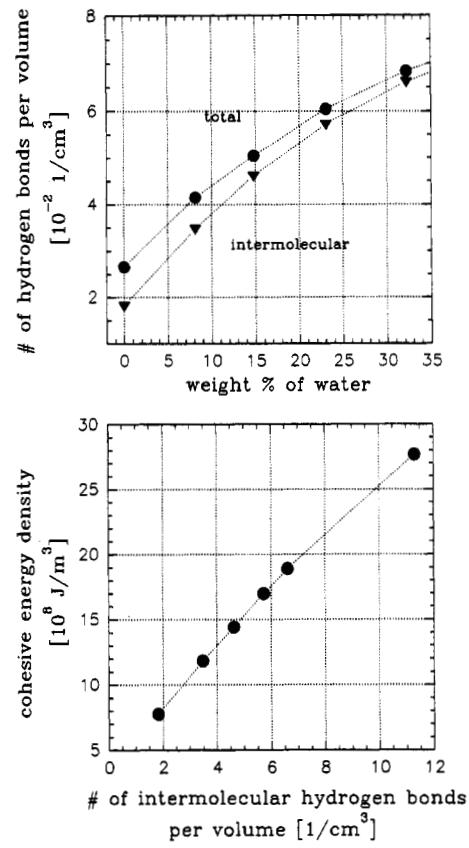

Figure 12. (a) Density of hydrogen bonds (total and *inter*molecular) as a function of the water content in the model structures. (b) Cohesive energy density as a function of the *inter*molecular hydrogen bond density (highest value: pure water).

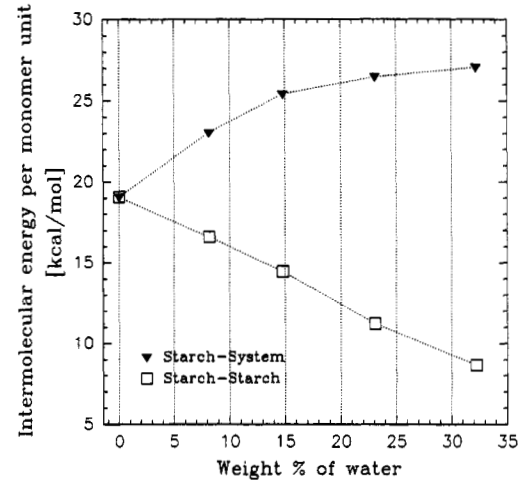

Figure 13. *Inter*molecular energy between the starch chains only and between the starch chain and the system in the model structures as a function of the water content.

respective mean values and standard deviations. Although there was a somewhat broader distribution at the lowest water content, no evidence could be found for especially bound waters. The mean energies as well as the standard deviations were constant irrespective of the water content.

The energy of evaporation was obtained by calculating the difference of the total *inter*molecular energy between structures of successive water content and dividing this quantity by the difference in the number of water molecules. From this value the energy of evaporation of pure water (determined from the energy-minimized

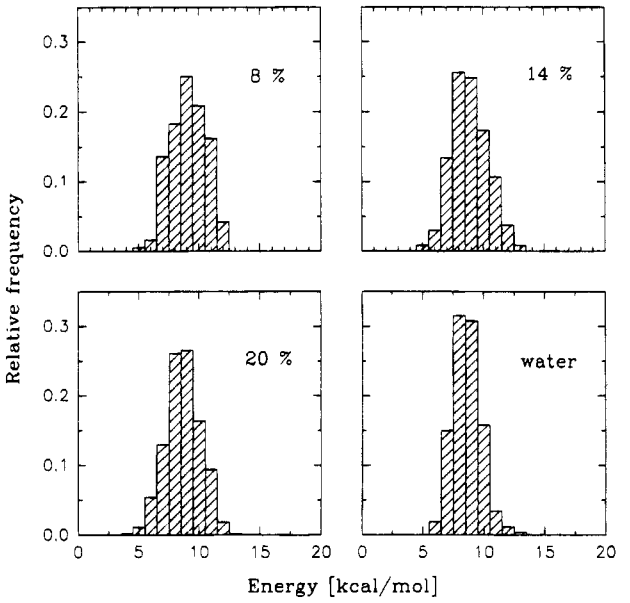

Figure 14. Histogram of the binding energies of the water molecules in the model structures with 8, 14, and 23% water and pure water.

Table 6. Mean Values and Standard Deviations of the Binding Energy of the Water Molecules in the Starch–Water Systems at Different Water contents

water content (%)	8	14	23	100
mean (kcal/mol)	-11.3 ± 1.4	-11.6 ± 1.5	-11.8 ± 1.4	-11.9 ± 1.2

water model structures) was subtracted to obtain the excess energy of evaporation (ΔE_{vap}^{exc}). ΔE_{vap}^{exc} decreased from 4.2 kcal/mol at low water content (<8.16%) to 0.4 kcal/mol at high water content (23.3–32.1%). In the intermediate ranges the values were 3.4 kcal/mol (8.16–14.3%) and 1.6 kcal/mol (14.3–23.3%). ΔE_{vap}^{exc} can be compared to experimental values of the excess enthalpy of evaporation, taking into account the contribution from the expansion of the gas, which amounts to $\sim RT$. The results compared well with the data of van den Berg (1981), who measured an excess enthalpy of 2.79 kcal/mol for the concentration range of 1.9–9.1% and 1.24 kcal/mol for the range of 9.1–16% of water in native starch.

Because no evidence has been found for stronger bound water molecules at lower water contents, the excess energy must be attributed to changes in the starch matrix upon the addition or taking away of water molecules. Signs for a change of the starch matrix were the decrease of *intra*molecular hydrogen bonds (Figure 9) found and the decrease in internal potential energies (Table 2) with increasing water content. Changes of the conformation of the chain with the water content with respect to the end-to-end distance and the distribution of the conformations among the two conformation angle regions were not detected (Table 3). To simulate such changes in the system with the highest water content, which is above T_g, much longer simulation times would be necessary due to the long relaxation times of the starch chain.

Mobility of the Water in the Starch Matrix. The term "bound" water, which has often been used in connection with polysaccharide–water interactions, can be interpreted in the sense of restricted mobility of the water molecules.[7] To investigate the dynamical behavior of the water molecules in the amorphous starch

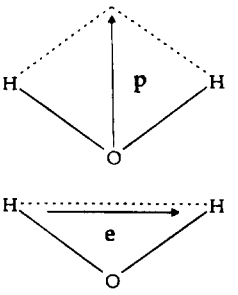

Figure 15. Definition of the vectors **p** and **e** to describe the movement of water molecules in the model structures.

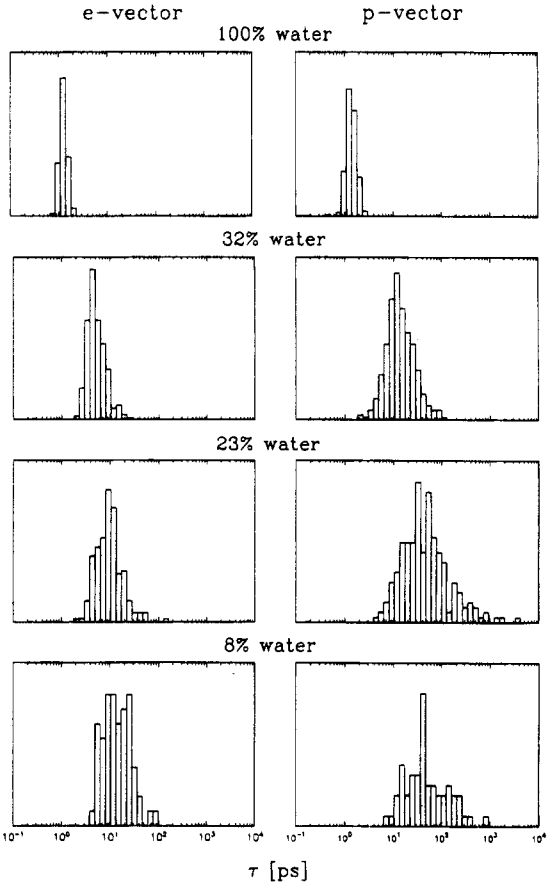

Figure 16. Distribution of correlation times of the vectors **p** and **e** in the starch structures at different water contents and in the pure water.

structure, a further simulation was made with selected microstructures. The movement of the water molecules was monitored during a molecular dynamics run at constant volume (*NVT*) for the period of 80 ps at 300 K. The time correlation functions of the vectors **p** and **e** that describe the rotation of the water molecule (see Figure 15) were calculated for every individual water molecule. They were fitted with an exponential decay function, $\exp(-t/\tau)$, and the distributions of correlation times, τ, are shown for the different model structures in Figure 16.

From the correlation time distributions, it can be seen that the movement of the water molecules in the starch matrix is hindered as compared to the situation in the pure water. This can be understood from the facts that (1) the water molecules are interacting with the starch chains via hydrogen bonds and (2) the starch chains are not moving during the simulation time period. Furthermore, a comparison between the correlation times of the **p** and **e** vectors showed that the movement of

the water molecules was anisotropic. This again can be explained by the hydrogen-bonding interaction between starch and water. The time correlation function of the **p** vector describes a rotation of the water about an axis perpendicular to **p**, and this requires a change of the direction of dipole moment of the water. The time correlation function of the **e** vector, however, contains the rotation of the water molecule about the axis parallel to the dipole moment, which does not change the direction of the dipole moment.

The correlation times of the **p** and **e** vectors showed a broad distribution, indicating a range of mobilities between almost liquid-like and solid-like waters. In the starch structures with a low water content, water molecules with correlation times that differ by 3 orders of magnitude were found. The mean correlation times decreased with increasing water content in starch. In the structure with the highest water content, the distribution was narrower, and water molecules with correlation times as high as those in the structures at low water contents were not found. All water molecules became gradually more mobile with increasing water content. The broad distribution of mobilities of the water molecules in starch indicated that very different local surroundings for the water exist, as might be expected from an amorphous structure.

From these results it can be concluded that the strong interactions between the water and the hydroxyl groups of the starch lead to stable geometrical arrangements that restrict the movement of the water molecules. Movements of the water molecule that require a change in the direction of the dipole moment were much more hindered than movements that preserve the dipole moment. Such anisotropic movement of the water molecules also has been found by proton NMR measurements.[15] A direct comparison of the relaxation times calculated from the model with relaxation times measured by NMR was not possible due to the complex interactions and the different protons involved. However, results of an NMR investigation have also shown that the mobility of the water increases gradually with increasing water content and that even at low water contents there is a distribution of mobilities.[19]

Chemical Potential of Water in the Amorphous Starch. The investigations on the structures of moist amorphous starch have shown that water was incorporated easily into the matrix and that it built up hydrogen bonds to the surroundings. It was shown that the water molecules are "bound" to the surroundings with the same energy as in ice. Their movements are hindered, as compared to the liquid water, and it was shown that the rotational diffusion of the water molecules displays a very broad distribution. Can the model reproduce the sigmoid sorption isotherm?

The excess chemical potential μ^{exc} of water has been evaluated for all starch–water structures at the different water contents. Figure 17 shows the results that were obtained for the individual microstructures (small filled symbols) and their averages (large filled symbols).

Following the course of the *mean* excess chemical potential, a strong increase was observed at low water contents and a leveling of the curve at higher water contents. Note, however, that the variation of the excess chemical potentials of the *individual microstructures* was large. The strong increase of μ^{exc} between the dry structure and that with 8% water was observed in all individual microstructures. At the higher water contents the trends of the individual μ^{exc} values differed and their change seemed to diminish.

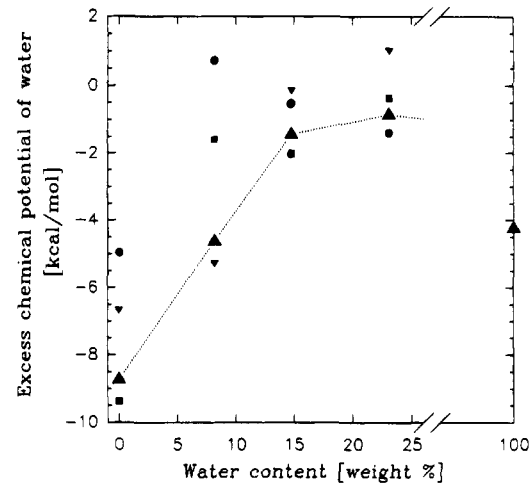

Figure 17. Modeled excess chemical potential of water in starch as a function of the water content. Large symbols are mean values and small symbols are the values evaluated for the individual microstructures.

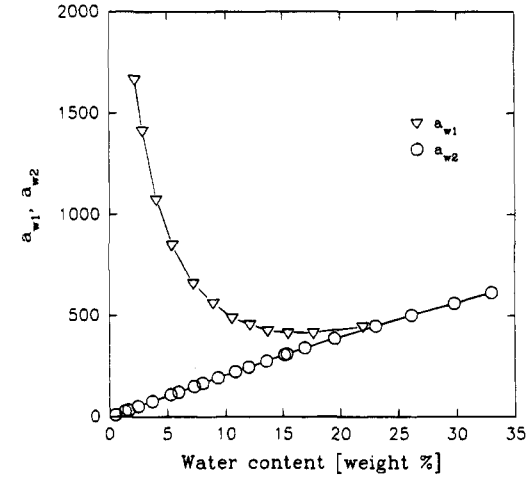

Figure 18. Components of the activity of water in starch derived from experimental data of Benczédi.[41] $a_{w1} = \langle \exp(-U_w/RT) \rangle$; $a_{w2} = \varrho_w^{starch}/\varrho_w^{id.gas}$. See text for further details.

The data on the starch–water systems presented in the last section have shown a low scattering of the qualities of the individual microstructures. The excess chemical potential is, however, strongly dependent on the interaction energies of the water with the matrix at the most favorable place(s) in the structure (see, e.g., eq 3). Since these interaction energies are large in the starch–water system, small geometrical changes are expected to result in large variations of μ^{exc}. To test this, the excess chemical potential was evaluated for the same microstructure, but varying the duration of the (*NVT*) molecular dynamics that was applied during the construction of the structure. It has been shown that this duration has very little effect on the cohesive energy or on the conformation of the chain. The additional run time was varied between 20 and 80 ps. As expected, the small changes in the positions of the atoms achieved by this method result in large variations—ca. 2 kcal/mol—of the excess chemical potential. Since the variation in μ^{exc} of the different microstructures was even larger (see Figure 18), the mean excess chemical potential should be calculated from a larger ensemble of microstructures.

In the dry structures the chemical potential was strongly negative; i.e., the solubility of water in starch is very high. Experimental data on the solubility for water are not available for starch. However, the Henry's constant for ethylcellulose, 2370 [cm^3(STP)/cm^3 atm],[55] might serve as a lower limit. The value calculated from the model structures is 10^6 [cm^3(STP)/cm^3 atm]. Although this value may be rather high, it confirms the experimental findings of the high affinity of starch for water. Dry starch is an excellent drying agent.

At high water contents, the system should increasingly resemble pure water. The excess chemical potential of pure water was evaluated from the model and amounts to −4.23 kcal/mol (energy-minimized water structure at the density of liquid water at 300 K). This value closely approximates the expected value of −4.3 kcal/mol, which can be calculated using eq 1, assuming chemical equilibrium between the ideal gas of water at 1 atm and bulk water at a density of 1 g/cm^3.

Taking the findings on the model calculations of the excess chemical potential of water in the starch−water system, the following results may be extracted. (1) In the dry structures the excess chemical potential of the water was low; i.e., the model predicts a strong affinity of the structure toward the water. (2) In the moist structures with intermediate water contents, μ^{exc} has increased considerably, but there was still an affinity of the system toward newly entering water. (3) In pure water the excess chemical potential has decreased again to an intermediate value. Here the agreement between expected and modeled values was good.

To compare these model data with experimental results and to address the question of whether the sigmoid shape of the water sorption isotherm of starch can be predicted from the model calculations, the activity of the water was decomposed according to eqs 1 and 2:

$$a_w = a_{w1} a_{w2}$$

$$a_{w1} = \varrho_w^{starch} / \varrho_w^{id,gas} \qquad (6)$$

$$a_{w2} = \frac{1}{\langle \exp(-U_w/RT) \rangle}$$

(since N_B is 1, ϱ_w^{starch} is practically the number density of water molecules in the starch matrix; $\varrho_w^{id,gas}$ is the number density of water in the ideal gas state).

Figure 18 shows the two components of eq 6 as derived from the experimental[41] (density and sorption) data. The sigmoid shape of the water sorption isotherm is reflected in the $\langle \exp(-U/RT) \rangle$ term and not in the density term. Figure 19 shows the excess chemical potential of the water in starch derived from experimental data.[41] A comparison of Figures 17 and 19 shows that from the model calculations the course of the excess chemical potential with the water content could be predicted. The model calculations thus also predicted the sigmoid shape of the sorption isotherm. However, the changes in the absolute values were much too large in the model and additional calculations are necessary to refine these findings. Note, furthermore, that the method used to generate the model structures models the system in the glassy state and the temperature entered *only* through the choice of the density. The starch−water system, however, is gradually plasticized by the water that enters the structure and its glass transition is lowered.[7,8] Therefore, it cannot be expected that the chemical potential can be calculated by this method for the entire concentration range of the starch−water system.

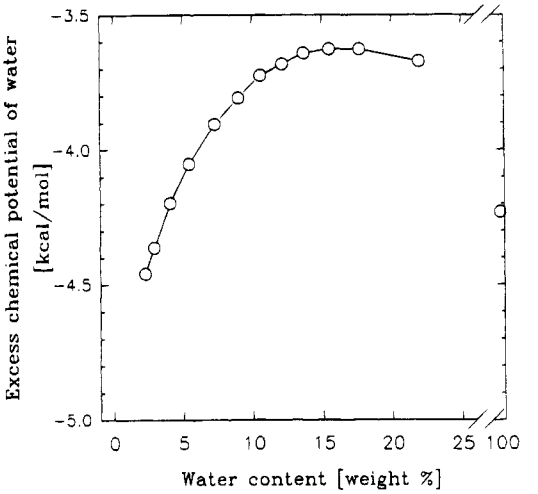

Figure 19. Experimental excess chemical potential of water in starch as a function of the water content derived from experimental data.[41]

Conclusions

The model of dry amorphous starch was extended to incorporate water. Structures were constructed with water contents ranging from 8 to 23%, which are typical for the starch−water system at ambient atmospheric conditions. They were used to interpret the measured differential radial distribution functions, to study the interactions of water and starch on a molecular level, and to understand the change of macroscopic properties like the cohesive energy density and the chemical potential with the water content. Furthermore, the influence of the starch matrix on the mobility of water has been investigated.

The radial distribution functions derived from the moist model structures and from X-ray scattering data of samples of amorphous starch (TPS) showed a good agreement with respect to the positions of the peaks up 5.5 Å. For higher distances, only qualitative agreement was found. The correlations of atoms within the repeat unit mainly determined the differential radial distribution function at low distances. They masked the *inter*molecular correlations and, therefore, changes in the differential radial distribution function—as measured with X-ray diffraction—with the amount of water in the system were small.

The interactions of the molecules in the starch−water system were found to be dominated by the interactions of the hydroxyl groups of the starch within themselves and with the water molecules. The possibilities to form hydrogen bonds were strongly augmented by the introduction of the small water molecule. On the macroscopic level, this was reflected in the increase of the cohesive energy density from 7.8×10^8 J/m^3 in the dry structures to 17×10^8 J/m^3 in the structures with 23% water. The correlation found in the dry starch structures between the cohesive energy density and the density of *inter*molecular hydrogen bonds was confirmed in the moist structures. On the microscopic level, a redistribution of the approximately 8 hydrogen bonds per repeat unit of starch with respect to *inter*- and

*intra*molecular hydrogen bonds was found. With increasing water content the number of starch-to-water hydrogen bonds increased, and the number of *intra*molecular hydrogen bonds decreased, both within a single repeat unit and within the same starch chain. Since the interaction energy in the starch–water system is coupled to the number of hydrogen bonds, this redistribution corresponds to a decrease in the interaction energy between the starch chains. Furthermore, because the water molecules are incorporated between the starch chains, the chains were moved further apart. The reduction of the *inter*action energy and the increase of the distance between the starch chains are both manifestations of the plasticizing effect of the water on the starch on a molecular level.

Parallel to the redistribution of the hydrogen bonds of the repeat units, a decrease of the contribution of the "internal" potential energy to the total potential energy of the system was found, indicating a relaxation of the repeat unit toward a less strained geometry.

The model structures allowed a detailed investigation of the hydrogen-bonding geometries and it was found that their geometry is highly variable and limited mainly by repulsive interactions. With increasing water content, a decrease was found in the amount of bifurcated donor hydrogen bonds. In the dry structures the deficit of hydrogen bond donors compared to acceptors was largest and most bifurcated donor hydrogen bonds were counted.

The water molecules that enter the amorphous starch structure were found to form 4 hydrogen bonds each to the surrounding, irrespective of whether the partner is starch or another water molecule. The energy with which they are bound in the matrix did not change with the water content, and no different classes of water could be detected from the distribution of the binding energies. All the same, the model structures confirmed that an excess energy is needed for the evaporation of water from starch. However, this excess energy cannot be attributed to a special binding situation of the water molecules and must therefore reflect changes in the starch matrix upon the addition or taking away of a water molecule.

The mobility of the water molecules was found to be restricted in the starch matrix as compared to the liquid water. The strong interactions between the water and the hydroxyl groups of starch hindered the movements of the water molecules that require a change in the direction of the dipole moment, i.e., the breaking of a hydrogen bond. The rotation of the water around the axis parallel to the direction of the dipole moment was less restricted. A broad distribution of mobilities of the water molecules was found with minimal and maximal correlation times differing by 3 orders of magnitude. The mean correlation times of the movements decreased with the water content. However, there was no evidence for the occurrence of two distinct classes of water molecules in this system. The results of these investigations corresponded to those already found by NMR measurements.

The high affinity of starch toward water could be confirmed by the calculations of the chemical potential of the water in the model structures. The chemical potential of the water was lowest in the dry structures and sharply increased at low water contents. In pure water it was found at an intermediate level; i.e., the chemical potential of the water in the starch–water system passed over a maximum value at a certain water content. The sigmoid shape of the measured water sorption isotherm of starch was thus predicted, although the absolute values of the excess chemical potential differed substantially from the experimental figures.

Acknowledgment. We gratefully acknowledge support by Grant No. 20-36291.92 of the Swiss National Fund for Scientific Research. We are also very grateful to Prof. U. W. Suter and his modeling group for many helpful discussions and support.

References and Notes

(1) Whistler, R. L. *Starch: Chemistry and Technology*; Whistler, R. L., Bemiller, J. N., Paschall, E. F., Eds.; Academic Press: New York, 1984; pp 1–9.
(2) Tomka, I.; Wittwer, F. Eur. Pat. Appl. 118240, P:51 pp, CL: C08L3/00, PRTY APPL:467982 (US), YR:1983 (18.02.83) PAT APPL:84/300940, YR:1984 (14.02.84), 1983.
(3) Tomka, I.; Stepto, R. F. T.; Dobler, B. Eur. Pat. Appl. 282451, P:9 pp, CL:C08B30/12, PRTY APPL:87/5442 (GB), YR:1987 (09.03.87) PAT APPL:88/810130, YR:1988 (02.03.88), 1987.
(4) Tomka, I.; Stepto, R. F. T.; Thoma, M. Eur. Pat. Appl. 304401, P:14 pp, CL:C08L3/02, PRTY APPL:87/19485 (GB), YR:1987 (18.08.87), PAT APPL:88/810548, YR:1988 (12.08.88), 1987.
(5) Willenbücher, R. W.; Tomka, I.; Müller, R. *Carbohydrates in Industrial Synthesis*; Proc. Symp. Div. Carb. Chem. Am. Chem. Soc.; Verlag Dr A. Bartens: Berlin, 1992; pp 93–111.
(6) van den Berg, C. Dissertation, Wageningen, The Netherlands, 1981.
(7) Sala, R. M.; Tomka, I. A. *Angew. Makromol. Chem.* **1992**, *199*, 45–63.
(8) Zeleznak, K. J.; Hoseney, R. C. *Cereal Chem.* **1987**, *64*, 121–124.
(9) Tomka, I. *Water Relationships in Foods*; Levine, H., Slade, L., Eds.; Plenum Press: New York, 1991; p 627–637.
(10) Levine, H.; Slade, L. *Water Relationships in Foods*; Plenum Press: New York, 1991.
(11) Blanshard, J. M. V.; Bates, D. R.; Muhr, A. H.; Worcester, D. L.; Higgins, J. S. *Carbohydr. Polym.* **1984**, *4*, 427–442.
(12) Slade, L.; Levine, H. *The Glassy State in Foods*; Blanshard, J. M. V.; Lillford, P. J., Eds.; Nottingham University Press: Nottingham, 1993; pp 35–102.
(13) Tomka, I. PRTY APPL:DE 4237 535.5 (06.11.92), 1992.
(14) van den Berg, C.; Kaper, F. S.; Weldring, J. A. G.; Wolters, I. *J. Food Technol.* **1975**, *10*, 589–602.
(15) Tanner, S. F.; Hills, B. P.; Parker, R. *J. Chem. Soc., Faraday Trans.* **1991**, *87*, 2613–2621.
(16) Noel, T. R.; Ring, S. R. *Carbohydr. Res.* **1992**, *227*, 203–213.
(17) Trommsdorff, U.; Tomka, I. *Macromolecules*, preceding paper in this issue.
(18) Orford, P. D.; Parker, R.; Ring, S. G.; Smith, A. C. *Int. J. Biol. Macromol.* **1989**, *11*, 91–96.
(19) Roosen, G. A. Dissertation, Hamburg, 1991.
(20) Baianu, I. C.; Kumosinski, T. F.; Bechtel, P. J.; Mora, A.; Kakalis, L. T.; Yakubu, P.; Myers-Betts, P.; Wei, T.-C. *Water Relations in Foods*; Levine, H., Slade, L., Eds.; Plenum Press: New York, 1991; pp 517–540.
(21) Delwiche, S. R.; Pitt, R. E.; Norris, K. H. *Starch/Stärke* **1991**, *43*, 415–422.
(22) Tomka, I. Dissertation, Bern, 1973.
(23) Grigera, J. R. *J. Chem. Soc., Faraday Trans. 1* **1988**, *84*, 2603–2608.
(24) Grigera, J. R. *Computer Modeling of Carbohydrates*; French, A. D., Brady, J. W., Eds.; ACS Symposium Series 430: American Chemical Society: Washington, DC, 1989; pp 152–161.
(25) Homans, S. W. *Biochemistry* **1990**, *29*, 9110–9118.
(26) Edge, C. J.; Singh, U. C.; Bazzo, R.; Taylor, G. L.; Dwek, R. A.; Rademacher, T. W. *Biochemistry* **1990**, *29*, 1971–1974.
(27) Kroon-Batenburg, L. M. J.; Kroon, J. *Biopolymers* **1990**, *29*, 1243–1248.
(28) van Eijck, B. P.; Kroon-Batenburg, L. M. J.; Kroon, J. *J. Mol. Struct.* **1990**, *237*, 315–325.
(29) Ha, S.; Gao, J.; Tidor, B.; Brady, J. W.; Karplus, M. *J. Am. Chem. Soc.* **1991**, *113*, 1553–1557.
(30) Eisenhaber, F.; Schulz, W. *Biopolymers* **1992**, *32*, 1643–1664.
(31) Jeffrey, G. A.; Saenger, W. *Hydrogen Bonding in Biological Structures*; Springer-Verlag: Berlin, 1991.
(32) Brady, J. W. *J. Am. Chem. Soc.* **1989**, *111*, 5155–5165.

(33) Brady, J. W.; Ha, S. N. *Water Relationships in Foods*; Levine, H., Slade, L., Eds.; Plenum Press: New York, 1991; pp 739–751.
(34) Madsen, L. J.; Ha, S. N.; Tran, V. H.; Brady, J. W. *Computer Modeling of Carbohydrates*; French, A. D., Brady, J. W., Eds.; ACS Symposium Series 430; American Chemical Society: Washington, DC, 1989; pp 69–90.
(35) Hardy, B. J.; Sarko, A. *J. Comput. Chem.* **1993**, *14*, 848–857.
(36) Köhler, J. E. H.; Sänger, W.; van Gunsteren, W. F. *J. Biomol. Struct. Dyn.* **1998**, *6*, 181–198.
(37) Brady, J. W.; Schmidt, R. K. *J. Phys. Chem.* **1993**, *97*, 958–966.
(38) Theodorou, D. N.; Suter, U. W. *Macromolecules* **1985**, *18*, 1467–1478.
(39) Maple, J.; Dinur, U.; Hagler, A. T. *Proc. Natl. Acad. Sci. U.S.A.* **1988**, *85*, 5350–5354.
(40) Maple, J. R.; Thacher, T. S.; Dinur, U.; Hagler, A. T. *Chem. Design Autom. News* **1990**, *5*, 5–10.
(41) Benzcédi, D., personal communication.
(42) Klug, H. P.; Alexander, L. E. *X-Ray Diffraction Procedures*; John Wiley & Sons: New York, 1974.
(43) Alexander, L. E. *X-Ray Diffraction Methods in Polymer Science*; R. E. Krieger Publishing Co.: Huntington, NY, 1985.
(44) Schubach, H. R. Dissertation, Ulm, 1984.
(45) Weber, K. *Acta Crystallogr.* **1967**, *23*, 720–725.
(46) Ben-Naim, A. *Statistical Thermodynamics for Chemists and Biochemists*; Plenum Press, New York, 1992.
(47) Widom, B. *J. Chem. Phys.* **1963**, *39*, 2808–2812.
(48) Allen, M. P.; Tildesley, D. J. *Computer Simulations of Liquids*; Clarendon Press: Oxford, 1992.
(49) Levesque, D.; Weiss, J. J. *The Monte Carlo Method In Condensed Matter Physics*; Binder, K., Ed.; Springer-Verlag: Berlin, 1991; p 172.
(50) Krynicki, K.; Green, C. D.; Sawyer, D. W. *Faraday Discuss. Chem. Soc.* **1978**, *66*, 199–208.
(51) Millane, R. P.; Arnott, S. *Water Relations in Foods*; Levine, H., Slade, L., Ed.; Plenum Press: New York, 1991; pp 785–803.
(52) Jeffrey, G. A. *Acta Crystallogr.* **1990**, *B46*, 89–103.
(53) Ceccarelli, C.; Jeffrey, G. A.; Taylor, R. *J. Mol. Struct.* **1981**, *70*, 255–271.
(54) Jeffrey, G. A.; Mitra, J. *Acta Crystallogr.* **1983**, *B39*, 469–480.
(55) *Polymer Handbook*. Brandrup, J., Immergut, E. H., Eds.; John Wiley & Sons: New York, 1989.
(56) *Handbook of Chemistry and Physics*. CRC Press: Boca Raton, FL, 1983–1984.
(57) Savage, H. F. J.; Finney, J. L. *Nature* **1986**, *322*, 717–720.

MA946349M